The Construction of (Salophen)ruthenium(II) Assemblies Using Axial Coordination

Kelly Chichak,[a] Ulrich Jacquemard,[a] and Neil R. Branda*[a,b]

Mononuclear and binuclear carbonylruthenium(II) complexes with N_2O_2 Schiff base ligands based on 3,5-di-*tert*-butylsalicylaldehyde and three different *ortho*-diamines have been prepared. The mononuclear Ru(BSP)(CO) [BSP = *N*,*N*′-bis(3,5-di-*tert*-butylsalicylidene)-1,2-phenylenediamine] complex **4** acts as a versatile supramolecular synthon, as illustrated by the fact that it spontaneously forms linear and three-dimensional assemblies through axial coordination with pyridyl Lewis bases. Using this motif, neutral and charged assemblies **6**, **9**, and **12** were prepared. The versatility of the salophen ligand was highlighted by the preparation of bimetallic carbonylruthenium(II) compounds **14–17** from 1,2,4,5-tetraaminobenzene and 2,3,7,8-tetraaminodibenzo-[1,4]dioxin. The bimetallic complexes were isolated as a mixture of *cis* and *trans* diastereomers with respect to the spatial relationship between the two axially bound carbon monoxide ligands. The electronic spectral and electrochemical properties of the pyridyl adducts **5**, **15**, and **17** were compared. The properties of **17** closely resembled **5** due to the insulating effect of the extended central tetraamino fragment, while **15** behaved as a single, novel chromophore. The electrochemical studies revealed that the central tetraamino linker regulates the communication between the two metal centers of **15** and **17**. It was found that the two metal atoms of **15** sense each other to a larger extent than those of **17**.

Introduction

The use of vacant axial coordination sites on metalloporphyrins in conjunction with substituted pyridines in order to create supramolecular assemblies with well-defined architectures and novel properties has been well exploited and extensively documented.[1] The construction of more elaborate porphyrin-based assemblies would provide access to new materials with tunable optical and electrochemical properties, suitable for modeling photosynthetic functions such as energy capture and transfer reactions, as well as new photonic devices such as solar cells and gated molecular circuitry.[2] However, there are significant shortcomings when substituted porphyrins are used. The syntheses tend to give low yields and it is tedious to isolate and purify the macrocycles, making the "design-to-realization" period for the highly functionalized porphyrin building blocks lengthy. Alternative molecular platforms that provide free binding sites suitable for axial coordination, which are more conducive to convenient synthesis, modification and isolation need to be explored.

Metallosalens **1** [salen = *N*,*N*′-bis(salicylidene)ethylenediamine] and metallosalophens **2** [salenophen = *N*,*N*′-bis-(salicylidene)-1,2-phenylenediamine] have received little attention as sources of planar supramolecular building blocks. These tetravalent ligands are particularly attractive for several reasons: 1) they are conveniently prepared in a single synthetic step by condensing substituted *ortho*-diamines with salicylaldehyde, and as a result, can be readily tailored by modifying the substituents on the diamine synthon; 2) they form stable coordination compounds with a wide variety of metal ions, which can be easily isolated; 3) if the appropriate metal ion is inserted into the ligands, the resulting complexes display accessible axial Lewis-acidic sites. Despite this appeal, we are aware of only one report describing the use of metallosalens or metallosalophens in the construction of multicomponent supramolecular assemblies through axial coordination. In this report, the authors describe how 4,4′-bipyridine axially coordinates to two methyl(salen)cobalt(III) complexes to produce a linear three-component assembly.[3]

1   **2**

Our recent success in constructing multicomponent assemblies using axial coordination to (porphyrin)ruthenium-
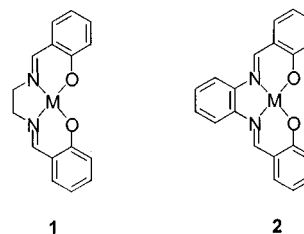
[a] Department of Chemistry, University of Alberta, Edmonton, Alberta, T6G 2G2, Canada
[b] Current address: Department of Chemistry, Simon Fraser University
8888 University Drive, Burnaby, B. C., V5A 1S6, Canada
Fax: (internat.) + 1-604/291-3765
E-mail: nbranda@sfu.ca

(II) synthons[4] prompted us to evaluate the versatility of the (salophen)ruthenium(II) analogues in supramolecular chemistry. The reported examples of axial coordination to carbonyl(salen)ruthenium(II) and carbonyl(salophen)ruthenium(II) complexes are limited in their scope and have certainly not been given the same degree of attention as their porphyrin counterparts. Here, we describe the application of the Ru(BSP)(CO) building block **4** [BSP = *N,N′*-bis(3,5-di-*tert*-butylsalicylidene)-1,2-phenylenediamine] in the generation of supramolecular linear and three-dimensional assemblies **6**, **9**, and **12**. The syntheses and characterization of bis(metallosalophen) complexes **14−17** are also reported.

Results and Discussion

Synthesis of the (Salophen)ruthenium(II) Building Block

In an early report involving metal−carbonyl insertion into salens, Calderazzo and co-workers describe the reaction of the unsubstituted ligand **1** (M = 2 H) with $Ru_3(CO)_{12}$ to produce a metallosalen dimer in high yield.[5] Owing to the insolubility of this dimeric product, it was characterized primarily using elemental analysis techniques, which gave the correct 1:1 metal-to-ligand stoichiometry for the coordination compound but not its three-dimensional structure. The authors postulated that the dimer is held together through axial coordination to the ruthenium center of each monomer by one of the Lewis basic oxygen atoms of the other. This claim was based on the fact that analogous iron(III) coordination compounds have been characterized in the solid state. In a later report, Farrell and co-workers described how the [Ru(**1**)(CO)]$_2$ dimer can be broken into its monomeric fragments only when heated in pyridine, where it dissociates to yield the pyridine-coordinated metallosalen monomer Ru(CO)(py)(salen).[6] Khan and co-workers described an alternative, milder approach to metal−carbonyl insertion, whereby a variety of chloro- and methoxy-substituted salens and salophens were treated with $Cs_2[RuCl_4(CO)(H_2O)]$.[7] To the best of our knowledge, the axial coordinating behavior of these chloro- and methoxy-substituted ruthenium(II) Schiff base complexes has not been reported.

In light of the dimerization product described by Calderazzo and Farrell, and the less than satisfactory structural and binding information on the reported metallo-Schiff base complexes, we sought a more soluble salophen ligand that is amenable to facile characterization in self-assembly processes. We chose *N,N′*-bis(3,5-di-*tert*-butylsalicylidene)-1,2-phenylenediamine (**3**) which precipitates as a yellow solid when 3,5-di-*tert*-butylsalicylaldehyde and 1,2-diaminobenzene are condensed in hot ethanol.[8] Metal insertion was accomplished by heating ligand **3** with an excess of $Ru_3(CO)_{12}$ in toluene (Scheme 1). Ru(BSP)(CO) (**4**) was isolated as a burgundy air-stable solid by a combination of column chromatography through activated alumina and recrystallization from aqueous ethanol. The isolation of **4** as a monomer was first suggested by the absence of signals
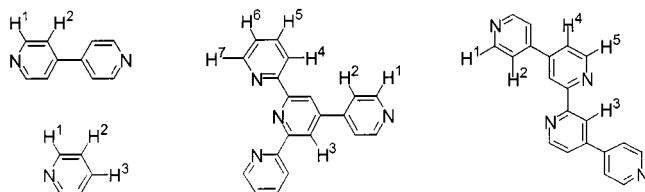
in the positive ion ES mass spectrum, corresponding to higher aggregates or multiply charged species, and then by the ease of forming axially coordinated supramolecular assemblies (see later). In addition to peaks corresponding to the parent ion (*m/z* = 668) and the loss of carbon monoxide (*m/z* = 640), the ES mass spectrum of a nitromethane solution of **4** contains peaks corresponding to the hydrated (*m/z* = 686) and solvated (*m/z* = 729 for [M + CH_3NO_2]$^+$) coordination compounds. We are assuming that the molecule of the solvent (CH_3NO_2 or H_2O) most likely occupies the axial site on the metal center. Clearly, the presence of the bulky *tert*-butyl substituents on the salophen ligand inhibits the dimerization of Ru(BSP)(CO) (**4**). Similar results have been reported for the zinc analogues of these types of coordination compounds.[9] Computer-assisted molecular modeling of **4** reveals that the sterically demanding *tert*-butyl substituents prevent the metallosalophens from approaching each other, thus inhibiting the formation of an analogous dimer to that originally reported by Calderazzo.
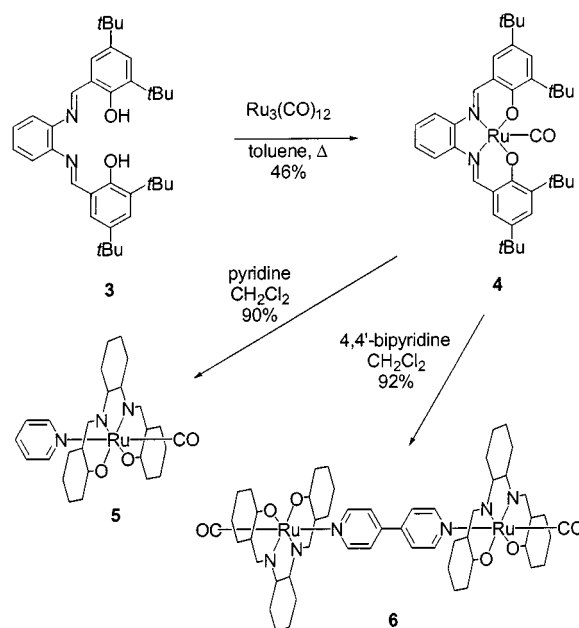
Scheme 1

The pyridine adduct Ru(BSP)(CO)(py) (**5**) was constructed when **4** was treated with an excess of pyridine in dichloromethane at room temperature. Compound **5** was isolated as a purple solid, by filtering the solution through silica gel which effectively removed any unchanged **4** as the pyridyl adduct is the only compound that elutes with CH_2Cl_2. The formation of **5** is confirmed by the upfield shifts (Δδ = −0.6 to −0.1) of the signals for the protons on the coordinated pyridine because these protons lie within the shielding regions of the aromatic rings of the salophen (Table 1). The generation of **5** using such mild conditions clearly indicates that, although the bulkiness of the *tert*-butyl substituents inhibits the dimerization of **4**, they do not impede the approach of Lewis bases such as pyridine towards the metal center. The ES mass spectrum

Table 1. Selected ^{1}H NMR spectroscopic data of the pyridyl-coordinated metallosalophen assemblies prepared in this study

Compound	δ ($\Delta\delta$)[a]						
	H[1]	H[2]	H[3]	H[4]	H[5]	H[6]	H[7]
5[b]	8.12 (−0.46)	7.09 (−0.18)	7.59 (−0.10)				
6[b]	8.19 (−0.52)	7.16 (−0.40)					
9a[c]	8.48 (−0.48)	8.16 (−0.13)	9.39 (−0.17)	7.63 (−0.20)	8.00 (−0.13)	7.21 (−0.15)	8.91 (−0.17)
9b[c]	8.53 (−0.47)	8.27 (−0.12)	9.55 (−0.20)	7.38 (−0.21)	7.95 (−0.13)	7.11 (−0.15)	8.27 (−0.12)
12a[c]	8.23 (−0.79)	7.58 (−0.66)	9.04 (−0.49)	7.45 (−0.62)	7.88 (−0.58)		
12b[c]	8.24 (−0.56)	7.59 (−0.33)	9.03 (−0.52)	7.56 (−0.47)	7.54 (−0.58)		
15[b] [d]	8.20 (−0.38)	7.16 (−0.11)	7.64 (−0.05)				
17[b] [d]	8.16 (−0.42)	7.14 (−0.13)	7.63 (−0.06)				

[a] Upfield shifts of the signals for the protons in the assemblies relative to those in free pyridine for assemblies **5**, **15** (*cis*) and **15** (*trans*), and **17** (*cis*) and **17** (*trans*), 4,4′-bipyridine for assembly **6**, complex **7** for assembly **9a**, tetrapyridine **8** for assembly **9b**, complex **10** for assembly **12a**, and tetrapyridine **11** for assembly **12b**. [b] In CH$_2$Cl$_2$. [c] In [D$_6$]acetone. [d] As a mixture of both *cis*- and *trans*-isomers.

of **5** shows a peak for the parent ion (*m/z* = 747), as well as peaks corresponding to the exchange of pyridine with a nitromethane solvent molecule (*m/z* = 729), to the loss of pyridine (*m/z* = 668) and to the loss of both axial ligands (*m/z* = 640). The intense band for ṽ(CO) in the IR spectrum of **5** is shifted to a higher frequency (1944 cm^{-1}) than that for **4** (1931 cm^{-1}), as is expected for the strengthening of the CO bond on addition of a π-acid.[10] The magnitude of this shift is comparable with that reported for the ṽ(CO) of the metallosalen **1** [M = Ru(CO)], as the [Ru(**1**)(CO)]$_2$ dimer is converted into its pyridine adduct.[6]

Construction of Neutral Assemblies

The use of the novel metallosalophen **4** as a supramolecular synthon was studied using ^{1}H NMR spectroscopy and then by the isolation of several air-stable multicomponent assemblies. A linear trimeric assembly [Ru(BSP)(CO)]$_2$(4,4′-bpy) (**6**) was prepared by treating a dichloromethane solution of 4,4′-bipyridine with 2.2 equiv. of Ru(BSP)(CO) (**4**) in the same solvent (Scheme 1). The ^{1}H NMR spectrum of **6**, whether generated in situ or isolated as described for **5**, shows the expected upfield shifts for the signals assigned to the protons of the coordinated 4,4′-bipyridine fragment (Figure 1 and Table 1). Our studies reveal that ligand exchange is slow on the NMR timescale and sharp peaks, that do not change, of the statistical mixture of mono- and di-

addition products are visible when 1.0 mol-equiv. of **4** is added (Figure 1). The ES mass spectrum of **6** exhibits a parent ion peak (*m/z* = 1492), as well as a peak (*m/z* = 824) corresponding to the loss of one metallosalophen. The spectrum also contains peaks that correspond to the fragmentation of the metallosalophen as previously seen for **4** and **5**. The IR spectrum of toluene solutions of **6** exhibits an intense band for ṽ(CO) at 1947 cm^{-1}.

Construction of Charged Assemblies

Metallosalophen assemblies incorporating coordination compounds as the central fragments were also prepared (Scheme 2). Addition of 2.0 mol-equiv. of Ru(BSP)(CO) (**4**) to the bis[4′-(4′′′-pyridyl)-2,2′:6′,2′′-terpyridine]ruthenium complex **7**[11] in acetone afforded the triad **9a**, which was isolated as a purple solid by precipitation with pentane. The iron analogue **9b** was readily synthesized from its simplest building blocks in a single self-assembly process, when equal parts of 4′-(4′′′-pyridyl)-2,2′:6′,2′′-terpyridine (**8**)[12] and Ru(BSP)(CO) (**4**) were added to an acetone solution containing 0.5 mol-equiv. of Fe(BF$_4$)$_2$(H$_2$O)$_6$. The ES mass spectra of both **9a** and **9b** each show parent ion peaks (*m/z* = 1028 for [M − 2 PF$_6$]$^{2+}$ and 1006 for [M − 2 BF$_4$]$^{2+}$), as well as peaks corresponding to the loss of one metallosalophen (*m/z* = 695 for [M − **4** − 2 PF$_6$]$^{2+}$ and 672 for [M − **4** − 2 BF$_4$]$^{2+}$). The IR spectrum for **9a** and
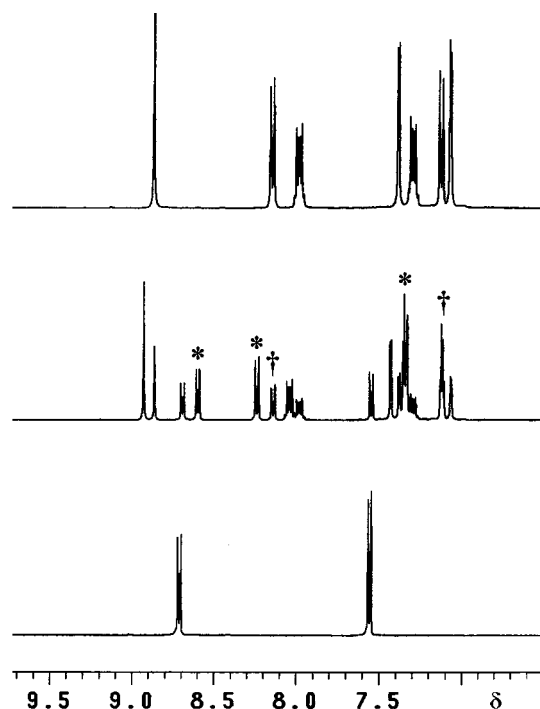
Figure 1. ^{1}H NMR (300 MHz) spectra of 4,4'-bipyridine (bottom trace), **4** + 1.0 equiv. of 4,4'-bipyridine (center trace), and **4** + 0.5 equiv. of 4,4'-bipyridine (top trace); signals corresponding to the protons of 4,4'-bipyridine for both the mono- (*) and the di-coordination (†) assemblies are highlighted; all spectra were run in CD$_2$Cl$_2$

9b obtained in the solid state exhibits intense bands for $\tilde{\nu}$(CO) at 1933 and 1934 cm^{-1}, respectively.

The syntheses of the octahedral ruthenium(II) and iron(II) assemblies **12a** and **12b** were accomplished according to our recently reported metal-directed synthesis employed to prepare the corresponding metalloporphyrin analogues (Scheme 2).[4a] The addition of [D$_6$]acetone to a 3:6:1 molar mixture of solid 4,4'-di(4''-pyridyl)-2,2'-bipyridine (**11**),[13] Ru(BSP)(CO) (**4**), and Fe(BF$_4$)$_2$(H$_2$O)$_6$, followed by 5 min of heating, cleanly afforded assembly **12b**. The octahedral assembly **12a** was prepared by treating the pre-assembled ruthenium(II) core fragment **10** with a slight excess of **4**. The ES mass spectra of both **12a** and **12b** each show a peak corresponding to the dications (m/z = 2519 for [M − 2 PF$_6$]$^{2+}$ and 2496 for [M − 2 BF$_4$]$^{2+}$, respectively), as well as peaks for the loss of subsequent metallosalophens. The IR spectra for **12a** and **12b** obtained in the solid state exhibit intense bands for $\tilde{\nu}$(CO) at 1947 and 1946 cm^{-1}, respectively.

Synthesis of Bis(salophens)

Illustrative examples that highlight the versatility of the salophen ligand are bis(metallosalophen) complexes **14**−**17**. These metallosalophens offer two accessible axial metal binding sites, separated by different intermetal distances based on the size of the tetraamine synthon (7.62 Å for **14** and **15**, and 12.32 Å for **16** and **17**). The corresponding

salophen ligands used to prepare these complexes were synthesized by condensing the 1,2,4,5-tetraaminobenzene hydrochloride salt for **14**, and the 2,3,7,8-tetraaminodibenzo-[1,4]dioxin hydrochloride salt **13**[14] for **16**, with 3,5-di-*tert*-butylsalicylaldehyde in ethanol under reflux (Scheme 3). Metal insertion was accomplished by heating the resulting salophens with Ru$_3$(CO)$_{12}$ in either toluene or diglyme, followed by purification using column chromatography through alumina. Complexes **14** and **16** were isolated as deep-red air-stable solids.

The ES mass spectrum of **14** shows the parent ion peak (m/z = 1258), as well as peaks corresponding to the solvated complex (m/z = 1336 for [M + H$_2$O + CH$_3$NO$_2$]$^+$, 1318 for [M + CH$_3$NO$_2$]$^+$ and 1370 for [M − CO + H$_2$O + 2 CH$_3$NO$_2$]$^+$). The ES mass spectrum of **16** shows a similar trend. The IR spectra for these bis(metallosalophens) obtained in the solid state exhibit intense bands for $\tilde{\nu}$(CO) at 1950 cm^{-1} for **14**, and at 1943 cm^{-1} for **16**.

The ^{1}H NMR spectrum of **14** in acetone reveals that the isolated product is a mixture of *cis* and *trans* diastereomers based on how the two carbonyl ligands project in space with respect to each other.[15] This is manifested as the appearance of two singlets of equal intensity assigned to the C−H protons on the central tetraaminobenzene ring fragment of **14**. The production of these stereoisomers is not unexpected, since the chelation sites are far away from each other so that they can act independently during the metal-insertion reactions. The diastereomeric mixture is even more apparent in the case of the pyridine adduct **15**, which was formed by treating complex **14** with pyridine, followed by the filtering of the solution through a plug of silica gel to remove trace amounts of unchanged **14**. The ^{1}H NMR spectrum of **15** shows an analogous pair of singlets assigned to the C−H hydrogen atoms on the central tetraaminobenzene fragment. The signals corresponding to the protons of the imine and flanking *tert*-butyl substituents on the bis(salophen) ligand, as well as C−H protons on the coordinated pyridine also appear as duplicate signals. These environmental effects are not limited to ^{1}H NMR spectroscopy, but are also apparent in the ^{13}C NMR spectrum for **15**, which contains duplicate signals for the coordinated pyridine ligand. On the other hand, the symmetrical nickel(II) analogue of **13** (Figure 2), prepared as a burgundy precipitate by treating the metal-free salophen ligand with 5 equiv. of Ni(OAc)$_2$(H$_2$O)$_4$, shows an absence of signal splitting in both the ^{1}H and ^{13}C NMR spectra (see Exp. Sect.).

The ^{1}H NMR spectra of the coordination compounds using the larger bis(metallosalophens) **16** and **17** show an absence of signal splitting for all protons, due to the greater separation between the two coordination sites. The ^{13}C NMR spectrum of **16** also lacks any signal splitting, however, the ^{13}C NMR spectrum of **17** exhibits two sets of signals corresponding to the coordinated pyridine ligands. All of the carbon atoms on the salophen ligand remain unaffected and appear as one set of signals. Again, the symmetrical nickel(II) analogue of **16** (Figure 2) does not show any multiple peaks in its NMR spectra.
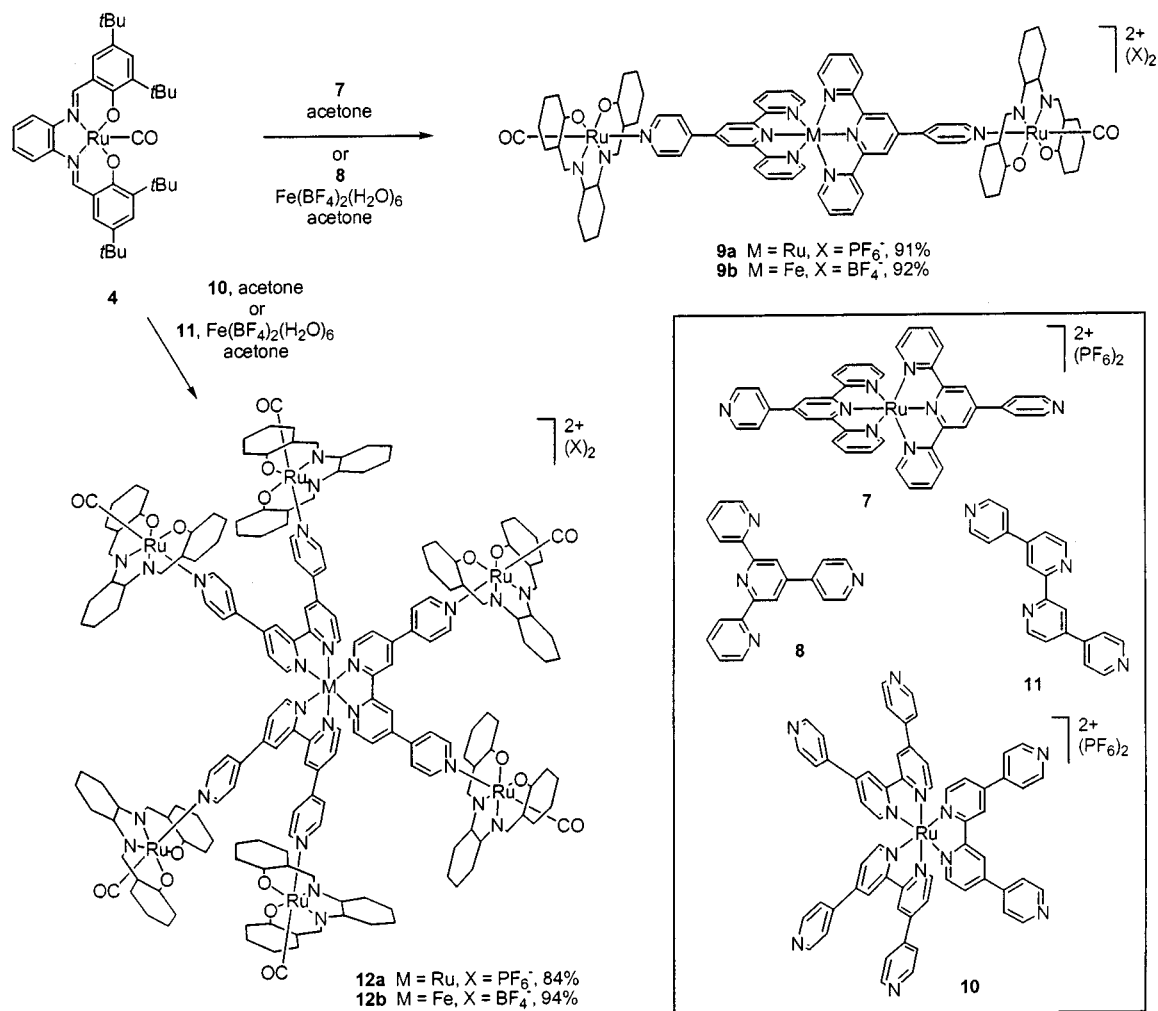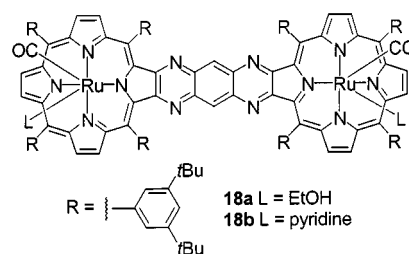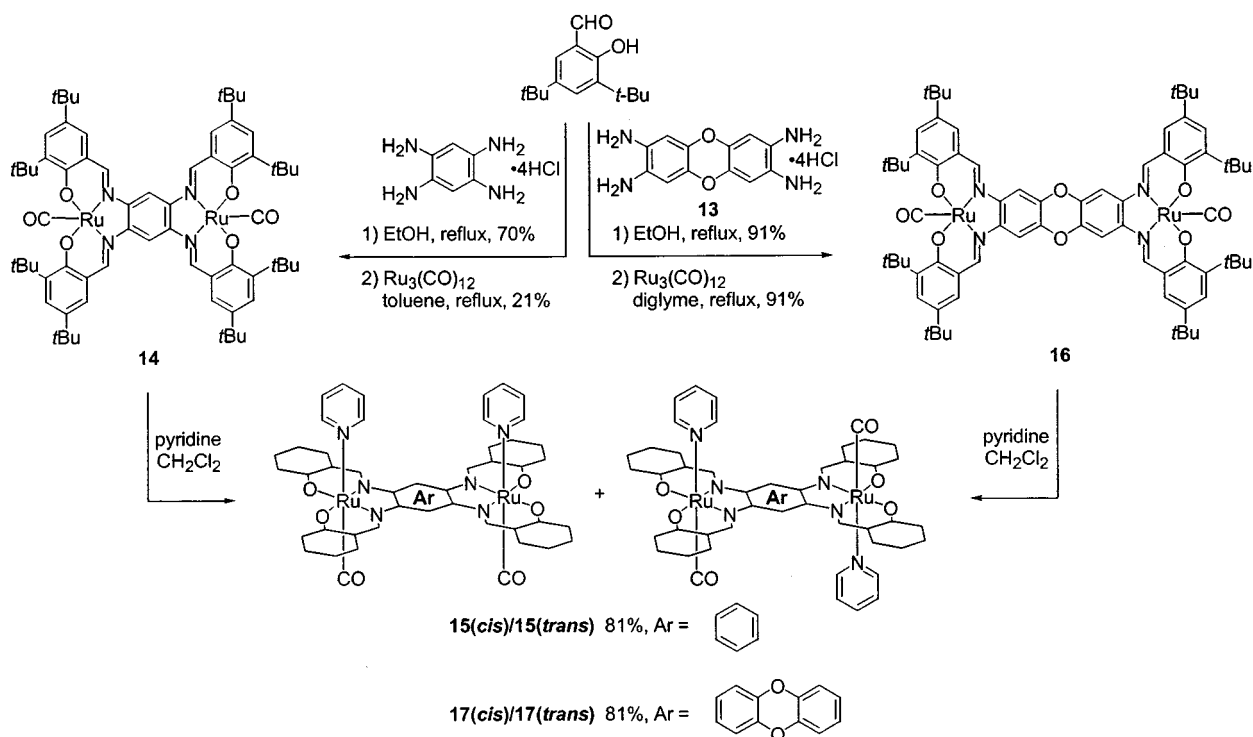
Scheme 2

The ES mass spectrum of **15** shows the parent ion peak ($m/z = 1416$) and peaks corresponding to the loss of pyridine ($m/z = 1338$ for $[M - py]^+$ and 1258 for $[M - 2 py]^+$). The ES mass spectrum of **17** shows a similar pattern. The IR spectra of the pyridine complexes **15** and **17** in the solid state show two intense overlapping bands for the stretching vibrations of the axial carbon monoxide (1955 cm^{-1} and 1924 cm^{-1} for **15**, 1951 cm^{-1} and 1934 cm^{-1} for **17**). The IR spectra measured in toluene exhibit two completely resolved $\tilde{\nu}$(CO) at 1944 cm^{-1} and 1924 cm^{-1} for **15**, and at 1947 cm^{-1} and 1934 cm^{-1} for **17**. A solvent dependency was also observed for the $\tilde{\nu}$(CO) of both pyridine complexes, and the IR spectra of dichloromethane solutions show a single band at 1940 cm^{-1} and 1931 cm^{-1} for **15** and **17**, respectively.

The convenience of incorporating the bis(metallosalophens) into supramolecular chemistry becomes clear when their syntheses are compared with that of the analogous bis(metalloporphyrin) **18a**. Although the metal insertion into Crossley's bis(porphyrin)[16] proceeded uneventfully by heating the bis(porphyrin) with an excess of Ru$_3$(CO)$_{12}$ in phenol, the preparation of the free-based porphyrin was ac-

complished in 5 steps giving a 50% yield as reported by Burn and co-workers.[17] This is a significant drawback when compared with our single-step preparation of the bis(salophen) precursor to **14**, and the two-step procedure for the precursor of **16**. The bis(metalloporphyrin) **18a** was purified as a brown air-stable solid by a combination of column chromatography through water-activated alumina and recrystallization from aqueous ethanol. When an excess of pyridine was added to **18a** in dichloromethane, the more Lewis-basic amine immediately displaced the labile ethanol affording the pyridine adduct.

Scheme 3

UV/Vis Spectroscopic Analysis

Initial photophysical studies reveal that UV/Vis absorption spectra of metallosalophen assemblies **6**, **9**, and **12** are essentially the sum of the absorption spectra of the corresponding components, and electronic absorptions are limited to minor shifts ($\Delta\lambda = \pm 2$ nm) (Table 2), although the steady-state emission spectra vary significantly (not shown). A more detailed description of the supramolecular absorption and emission properties of the metallosalophen assemblies will be the subject of a separate report.

The absorption spectra of dichloromethane solutions of **5**, **15** (as the mixture of *cis* and *trans* isomers), and **17** (as the mixture of *cis* and *trans* isomers) are characterized by intense ligand-centered (LC) bands with maxima in the 250−400 nm region (Figure 3).[7,18] These bands have been designated as $\pi-\pi^*$ and $n-\pi^*$ transitions for the electrons localized on the azomethine group of the Schiff base ligand. The bands at longer wavelengths are most likely due to ligand(π)−metal(d*) charge transfer, as has been reported for similar complexes.[7,18a,18c] The similarity of the electronic spectra of complexes **5** and **17** suggests that the central dibenzodioxin fragment effectively separates the metal centers from each other, allowing them to act independently. However, this effect does not apply to complex **15**, which exhibits a unique pattern of red-shifted charge-transfer bands. This observation is indicative of the fact that **15** is behaving as one extended chromophore and not as two independent metallosalophens.

Electrochemistry of Bis(salophens)

The cyclic voltammograms of dichloromethane solutions of complexes **5**, **15** (as the mixture of *cis* and *trans* isomers), and **17** (as the mixture of *cis* and *trans* isomers) do not show any reduction waves at negative potentials, but do show two quasi-reversible ($\Delta E = 70-90$ mV) oxidation waves centered at 0.58 V (assigned as a Ru^{II}/Ru^{III} process) and 1.29 V (assigned as a Ru^{III}/Ru^{IV} process) vs. saturated Ag/AgCl (Figure 4).[18a] For the scan rates used, the cathodic-to-anodic peak current ratio (i_{pc}/i_{pa}) is constantly equal to unity for the first oxidation and slightly less than unity for the second oxidation; the quotient of the anodic peak current and the square root of the scan rate ($i_{pa}/v^{1/2}$) remains constant. Complex **5** is well behaved, showing two one-electron oxidations at 0.56(7) and 1.29(4) V. For the bimetallic species **15** and **17**, the first oxidation waves are two-electron processes [actually, two one-electron oxidations at each ruthenium(II) center] and are shifted to slightly more positive potentials [0.60(0) and 0.58(2) V for **15** and **17**, respectively]. This indicates that the metal centers do not communicate with each other for the Ru^{II}/Ru^{III} couple. The second oxidation wave of the bimetallic species are split into two one-electron oxidation waves at 1.27(7)/1.36(8) V for **15** and 1.28(4)/1.33(0) for **17**, indicative of weak interactions between the covalently linked metallosalophens. This metal-to-metal communication is amplified in the case of the smaller complex **15** ($\Delta V = 91$ mV), as compared with the larger complex **17** ($\Delta V = 50$ mV).
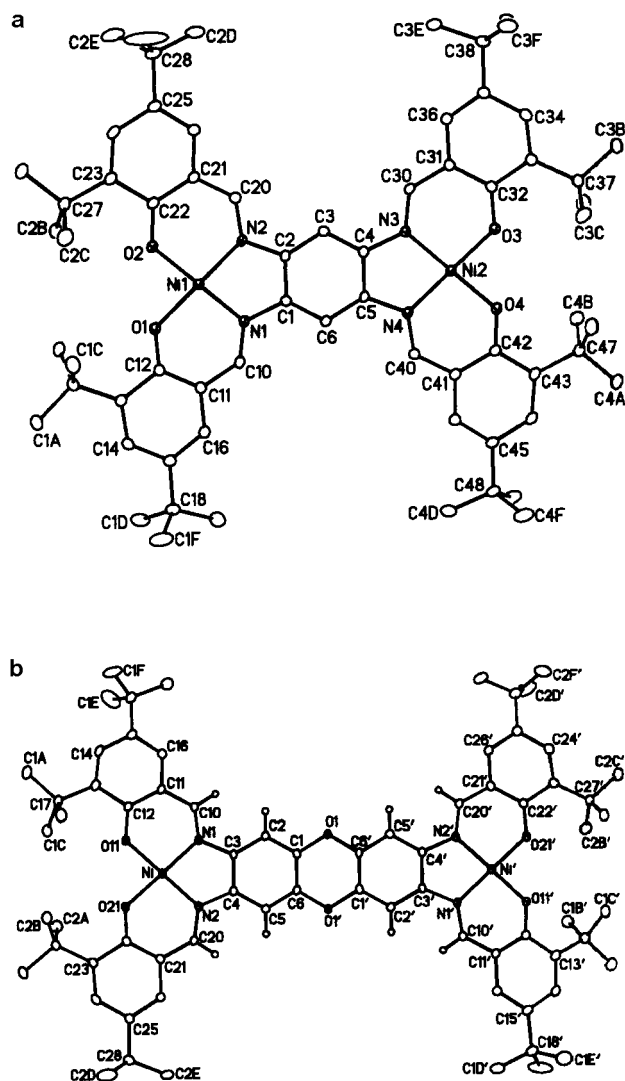
Figure 2. Molecular structures of the nickel(II) analogues of (a) **14** and (b) **16** in the crystal; solvent molecules (acetone/CH₂Cl₂ for **14** and THF for **16**) have been removed for clarity; the thermal ellipsoids are drawn at the 20% probability level

Table 2. Selected UV/Vis absorption data of the pyridyl-coordinated metallosalophen assemblies prepared in this study

Compound	λ_{max} [nm] (log ε [$M^{-1}cm^{-1}$])[a]					
4	258	306	382	491	541[b]	
	(4.48)	(4.26)	(4.38)	(3.91)	(3.75)	
5	264	310	391	503	555[b]	
	(4.68)	(4.38)	(4.60)	(4.02)	(3.09)	
6	264	310	391	501	555[b]	
	(4.81)	(4.56)	(4.70)	(4.17)	(4.00)	
9a	276	312	330	390	493	555[b]
	(5.01)	(4.88)	(4.77)	(4.74)	(4.59)	(4.18)
9b	282	291	327	393	508	573[b]
	(5.02)	(5.02)	(4.82)	(4.75)	(4.35)	(4.52)
12a	255	311	388	490	555[b]	
	(5.34)	(5.19)	(5.18)	(4.77)	(4.53)	
12b	285	311	391	506	555[b]	
	(5.39)	(5.16)	(5.21)	(4.72)	(4.70)	
15[c]	313	325	407	492	551[b]	614[b]
	(4.58)	(4.57)	(4.62)	(4.42)	(4.37)	(4.35)
17[c]	263	304	317	400	520	566[b]
	(4.75)	(4.70)	(4.70)	(4.80)	(4.29)	(4.22)

[a] Run in deoxygenated CH₂Cl₂ at 10^{-4} to 10^{-5} M. [b] Observed as a shoulder. [c] As a mixture of both *cis* and *trans* isomers.
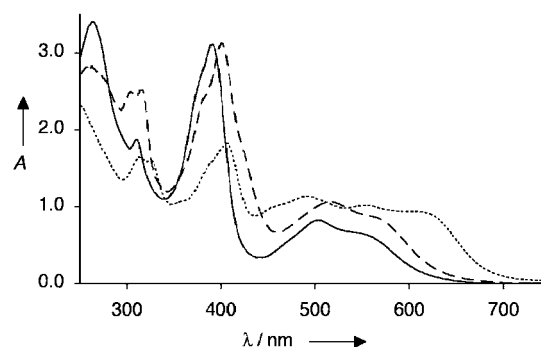

Figure 3. UV/Vis absorption spectra of Ru(BSP)(CO)(py) (**5**) (solid line), Ru₂[(BS2P)(CO)₂(py)₂] (**15**, both isomers) (dotted line), and Ru₂[(BS2DP)(CO)₂(py)₂] (**17**, both isomers) (dashed line) in CH₂Cl₂ at room temperature

Conclusion

In summary, this work highlights the fact that mononuclear and binuclear ruthenium(II) carbonyl Schiff base complexes can be prepared in a facile manner from *ortho*-diamines and 3,5-di-*tert*-butylsalicylaldehyde. We have also established that Ru(BSP)(CO) (**4**) has the same axial coordination properties as our previously reported Ru(CO)-(TTP) supramolecular synthons. The ease with which salophens can be modified represents a significant synthetic advantage over its metalloporphyrin analogue, as was demonstrated by the formation of the carbonylbis(metallosalophens)ruthenium(II). The ease of synthetically tailoring the *ortho*-diamine synthon of the salophen ligands should spark efforts to further develop this class of supramolecular building blocks.

Experimental Section

General Remarks: All solvents (Caledon) were distilled prior to use. Solvents used for UV/Vis spectroscopy were deoxygenated by bubbling argon through the solvent. Solvents for NMR analysis (Cambridge Isotope Laboratories) were used as received. All reagents and starting materials were purchased from Aldrich. *N,N′*-Bis(3,5-di-*tert*-butylsalicylidene)-1,2-phenylenediamine (**3**),[8] [Ru(p-ytpy)₂][PF₆]₂ (**7**)[11] [pytpy = 4′-(4′′′-pyridyl)-2,2′:6′,2′′-terpyridine], 4′-(4′′′-pyridyl)-2,2′:6′,2′′-terpyridine (**8**),[12] [Ru(dpyb-py)₃][PF₆]₂ (**10**)[4a] [dpybpy = 4,4′-di(4′′-pyridyl)-2,2′-bipyridine], and 4,4′-di(4′′-pyridyl)-2,2′-bipyridine (**11**)[13] were prepared as described in the literature. ¹H NMR characterizations were performed with a Varian Inova-500 instrument, working at 499.92 or with a Varian Inova-300 instrument, working at 299.96 MHz. Chemical shifts (δ) are reported in ppm relative to tetramethylsilane using the residual solvent peak as a reference standard. FT-IR measurements were performed using a Nicolet Magna-IR 750
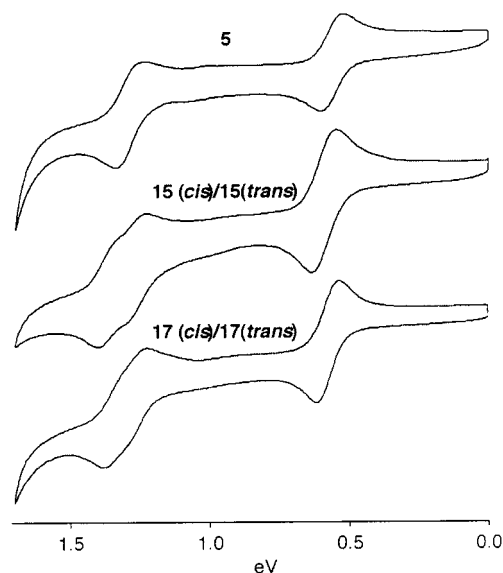
Figure 4. Cyclic voltammograms of (a) Ru(BSP)(CO)(py) (**5**), (b) Ru$_2$[(BS2P)(CO)$_2$(py)$_2$] (**15**, both isomers), and (c) Ru$_2$[(BS2DP)(CO)$_2$(py)$_2$] (**17**, both isomers) at identical scan rates of 50 mV/s in CH$_2$Cl$_2$ with 0.1 M TBAP at room temperature

microscope. UV/Vis measurements were performed using a Varian Cary 400 Scan spectrophotometer. Cyclic voltammetry measurements were performed in CH$_2$Cl$_2$ using a PINE bipotentiostat, a platinum working electrode, a platinum counter electrode and an Ag/AgCl reference electrode, and tetrabutylammonium hexafluorophosphate as the electrolyte. MALDI mass spectra were recorded with an Applied Biosystems Voyager Elite equipped with delayed extraction and an ion mirror (reflectron). Electrospray ionization mass spectra were recorded with a Micromass ZabSpec Hybrid Sector-TOF with positive mode electrospray ionization. All isotopic abundances match the calculated values.

Ru(BSP)(CO) (4): A solution of *N,N'*-bis(3,5-di-*tert*-butylsalicylidene)-1,2-phenylenediamine (**3**) (130 mg, 0.242 mmol) and Ru$_3$(CO)$_{12}$ (65.0 mg, 0.102 mmol) in toluene (5 mL) was heated under reflux for 15 h under argon. The reaction mixture was cooled to room temperature, filtered through Celite, and concentrated under reduced pressure. The resulting dark red residue was chromatographed on alumina (II−III) eluting first with toluene to remove an orange band, followed by CH$_2$Cl$_2$ to remove a yellow band, and then with a mixture of EtOH/CH$_2$Cl$_2$ (5:95) to remove a red-pink band. The red-pink band was concentrated to dryness under vacuum affording **4** as a glassy red solid that was recrystallized from aqueous EtOH. Yield: 73 mg (46%). ^{1}H NMR (300 MHz, [D$_6$]acetone, 22 °C): δ = 9.34 (s, 2 H), 8.29 (dd, *J* = 3.3, 9.6 Hz, 2 H), 7.48 (d, *J* = 2.7 Hz, 2 H), 7.40 (d, *J* = 2.7 Hz, 2 H), 7.33 (dd, *J* = 3.3, 9.6 Hz, 2 H), 1.55 (s, 18 H), 1.33 (s, 18 H). ^{13}C NMR APT (125.7 MHz, [D$_6$]acetone, 22 °C): δ = 170.6 (C), 157.2 (CH), 146.9 (C), 142.7 (C), 135.2 (C), 131.0 (CH), 130.1 (CH), 126.7 (CH), 121.7 (C), 116.1 (CH), 36.6 (C), 34.5 (C), 31.7 (CH$_3$), 30.4 (CH$_3$). HRMS (ES+): *m/z* = 668.2552 [M$^+$]. Selected IR: ṽ = 1931 (CO) cm^{-1}.

Ru(BSP)(CO)(py) (5): A solution of pyridine (0.25 mL) in CH$_2$Cl$_2$ (5 mL) was treated with Ru(BSP)(CO) (**4**) (38.0 mg, 0.055 mmol) and stirred at room temperature for 30 min. Silica gel (1 g) was added and the solvents were evaporated. The solid residue was ap-

plied to a small column of silica gel (1 × 2 cm) and eluted with CH$_2$Cl$_2$. The first band was collected and concentrated to dryness affording **5** as a purple solid. Yield: 37 mg (90%). ^{1}H NMR (300 MHz, CD$_2$Cl$_2$, 22 °C): δ = 8.90 (s, 2 H), 8.12 (m, 2 H), 8.01 (dd, *J* = 3.3, 9.9 Hz, 2 H), 7.59 (m, 1 H), 7.42 (d, *J* = 2.7 Hz, 2 H), 7.32 (dd, *J* = 3.3, 9.6 Hz, 2 H), 7.09 (m, 4 H), 1.56 (s, 18 H), 1.28 (s, 18 H). ^{13}C NMR APT (125.7 MHz, CD$_2$Cl$_2$, 22 °C): δ = 170.0 (C), 155.0 (CH), 149.5 (CH), 145.9 (C), 143.0 (C), 138.0 (CH), 135.1 (C), 130.1 (CH), 130.0 (CH), 126.2 (CH), 124.6 (CH), 120.5 (C), 115.1 (CH), 36.3 (C), 34.1 (C), 31.4 (CH$_3$), 29.9 (CH$_3$). HRMS (ES+): *m/z* = 747.2974 [M$^+$]. Selected IR: ṽ = 1942 (CO) cm^{-1}.

[Ru(BSP)(CO)]$_2$[4,4′-bipy] (6): A solution of 4,4′-bipyridine (3.9 mg, 0.025 mmol) in CH$_2$Cl$_2$ (5 mL) was treated with Ru(BSP)(CO) (**4**) (35.0 mg, 0.051 mmol) and stirred at room temperature for 30 min. Silca gel (1 g) was added and the solvents were evaporated. The solid residue was applied to a small column of silica gel (1 × 2 cm) and eluted with CH$_2$Cl$_2$. The first band was collected and concentrated to dryness affording **6** as a purple solid. Yield: 34.0 mg (92%). ^{1}H NMR (300 MHz, CD$_2$Cl$_2$, 22 °C): δ = 8.91 (s, 4 H), 8.19 (dd, *J* = 1.5, 6.6 Hz, 4 H), 8.02 (dd, *J* = 3.6, 9.9 Hz, 4 H), 7.43 (d, *J* = 2.4 Hz, 4 H), 7.34 (dd, *J* = 3.3, 9.6 Hz, 4 H), 7.16 (dd, *J* = 1.5, 6.6 Hz, 4 H), 7.11 (d, *J* = 2.4 Hz, 4 H), 1.50 (s, 36 H), 1.27 (s, 36 H). ^{13}C NMR APT (125.7 MHz, CD$_2$Cl$_2$, 22 °C): δ = 169.9 (C), 155.1 (CH), 150.3 (CH), 146.4 (C), 145.8 (C), 143.0 (C), 135.2 (C), 130.0 (CH), 126.1 (CH), 122.4 (CH), 120.5 (C), 115.1 (CH), 36.2 (C), 34.1 (C), 31.3 (CH$_3$), 29.9 (CH$_3$). MS (ES+): *m/z* = 1492 [M$^+$]. Selected IR: ṽ = 1938 (CO) cm^{-1}.

[Ru(BSP)(CO)]$_2$[Ru(pytpy)$_2$][PF$_6$]$_2$ (9a): A solution of [Ru(pytpy)$_2$][PF$_6$]$_2$ (**7**)[11] (2.2 mg, 2.2 μmol) in acetone (5 mL) was treated with Ru(BSP)(CO) (**4**) (3.4 mg, 5.0 μmol) and stirred at room temperature for 30 min. The solvents were evaporated and the resulting solid was triturated in a mixture of Et$_2$O/pentane (20:80) and dried under vacuum. Yield: 4.7 mg (91%). ^{1}H NMR (300 MHz, [D$_6$]acetone, 22 °C): δ = 9.40 (s, 4 H), 9.39 (s, 4 H), 8.91 (d, *J* = 8.1 Hz, 4 H), 8.48 (d, *J* = 6.6 Hz, 4 H), 8.39 (dd, *J* = 3.6, 9.9 Hz, 4 H), 8.17 (d, *J* = 6.6 Hz, 4 H), 8.00 (t, *J* = 7.8 Hz, 4 H), 7.63 (d, *J* = 4.8 Hz, 4 H), 7.50 (d, *J* = 2.4 Hz, 4 H), 7.40 (m, 8 H), 7.21 (t, *J* = 6.0 Hz, 4 H), 1.61 (s, 36 H), 1.32 (s, 36 H). MS (ES+): *m/z* = 1028 [M − 2 PF$_6$]$^{2+}$. Selected IR: ṽ = 1933 (CO) cm^{-1}.

[Ru(BSP)(CO)]$_2$[Fe(pytpy)$_2$][BF$_4$]$_2$ (9b): A solid mixture of 4′-(4‴-pyridyl)-2,2′:6′,2″-terpyridine (**8**)[12] (3.1 mg, 0.01 mmol), Fe(BF$_4$)$_2$(H$_2$O)$_6$ (1.7 mg, 5.0 μmol), and Ru(BSP)(CO) (**4**) (15.0 mg, 0.022 mmol) was dissolved in acetone (5 mL) and stirred at room temperature for 30 min. The solvents were evaporated and the resulting solid product was triturated in a mixture of Et$_2$O/pentane (20:80) and dried under vacuum. Yield: 20.1 mg (92%). ^{1}H NMR (300 MHz, [D$_6$]acetone, 22 °C): δ = 9.56 (s, 4 H), 9.42 (s, 4 H), 8.86 (d, *J* = 7.8 Hz, 4 H), 8.53 (d, *J* = 6.6 Hz, 4 H), 8.40 (dd, *J* = 3.3, 9.6 Hz, 4 H), 8.27 (d, *J* = 6.6 Hz, 4 H), 7.95 (t, *J* = 7.8 Hz, 4 H), 7.50 (d, *J* = 2.4 Hz, 4 H), 7.40 (m, 12 H), 7.11 (t, *J* = 6.0 Hz, 4 H), 1.63 (s, 36 H), 1.32 (s, 36 H). MS (ES+): *m/z* = 1006 [M − 2 BF$_4$]$^{2+}$. Selected IR: ṽ = 1934 (CO) cm^{-1}.

[Ru(BSP)(CO)]$_6$[Ru(dpybpy)$_3$][PF$_6$]$_2$ (12a): A solution of [Ru(dpybpy)$_3$][PF$_6$]$_2$ (**10**)[4a] (2.0 mg, 1.5 mmol) in acetone (5 mL) was treated with Ru(BSP)(CO) (**4**) (6.4 mg, 9.6 mmol) and stirred under reflux for 30 min. The solvents were evaporated and the resulting solid product was triturated in a mixture of Et$_2$O/pentane (20:80) and dried under vacuum. Yield: 6.8 mg (84%). ^{1}H NMR (500 MHz, [D$_6$]acetone, 22 °C): δ = 9.27 (s, 12 H), 9.04 (s, 6 H), 8.31 (m, 12

H), 8.23 (d, J = 6.5 Hz, 12 H), 7.88 (d, J = 6.0 Hz, 6 H), 7.58 (d, J = 6.5 Hz, 12 H), 7.45 (m, 18 H), 7.38 (dd, J = 3.5, 9.5 Hz, 12 H), 7.30 (s, 12 H), 1.55 (s, 108 H), 1.30 (s, 108 H). MS (ES+): m/z = 2519.5 [M − 2 PF$_6$]$^{2+}$. Selected IR: $\tilde{\nu}$ = 1946 (CO) cm^{-1}.

[Ru(BSP)(CO)]$_2$[Fe(dpybpy)$_2$][BF$_4$]$_2$ (12b): A solid mixture of 4,4′-di(4′′-pyridyl)-2,2′-bipyridine (**11**)$^{[13]}$ (1.2 mg, 3.9 μmol), Fe(BF$_4$)$_2$(H$_2$O)$_6$ (0.5 mg, 1.5 μmol), and Ru(BSP)(CO) (**4**) (6.5 mg, 9.5 μmol) was dissolved in acetone (5 mL) and stirred under reflux for 30 min. The solvents were evaporated and the resulting solid product was triturated in a mixture of Et$_2$O/pentane (20:80) and dried under vacuum. Yield: 7.1 mg (94%). ^{1}H NMR (500 MHz, [D$_6$]acetone, 22 °C): δ = 9.28 (s, 12 H), 9.03 (s, 6 H), 8.32 (m, 12 H), 8.24 (d, J = 7.0 Hz, 12 H), 7.59 (d, J = 7.0 Hz, 12 H), 7.56 (dd, J = 1.5, 6.0 Hz, 6 H), 7.54 (d, J = 6.0 Hz, 6 H) 7.45 (m, 12 H), 7.38 (dd, J = 3.5, 10.0 Hz, 12 H), 7.31 (d, J = 2.5 Hz, 12 H), 1.57 (s, 108 H), 1.31 (s, 108 H). MS (ES+): m/z = 2496.5 [M − 2 BF$_4$]$^{2+}$. Selected IR: $\tilde{\nu}$ = 1946 (CO) cm^{-1}.

***N*,*N*′′,*N*′′′,*N*′′′′-Tetra-(3,5-di-*tert*-butylsalicylidene)-1,2,4,5-phenylenetetraamine [Bis(salophen) Precursor to 14] (BS2P):** 3,5-Di-*tert*-butylsalicylaldehyde (1.00 g, 4.27 mmol) and 1,2,4,5-benzenetetramine tetrahydrochloride (250 mg, 0.880 mmol) were heated in EtOH (5 mL) under reflux for 15 h. The solution was cooled to −10 °C and stirred for 3 h. The yellow-orange precipitate was collected by filtration, washed with EtOH and dried under vacuum. Yield: 610 mg (70%). M.p. 285−286 °C. ^{1}H NMR (360 MHz, CD$_2$Cl$_2$, 27 °C): δ = 13.53 (s, 4 H), 8.83 (s, 4 H), 7.49 (d, J = 2.2 Hz, 4 H), 7.32 (d, J = 2.3 Hz, 4 H), 7.25 (s, 4 H), 1.52 (s, 36 H), 1.33 (s, 36 H). ^{13}C NMR APT (125.7 MHz, CDCl$_3$, 27 °C): δ = 164.7 (CH), 158.7 (C), 141.6 (C), 140.6 (C), 137.3 (C), 128.6 (CH), 127.0 (CH), 118.4 (C), 111.2 (CH), 35.2 (C), 34.1 (C), 31.5 (CH$_3$), 29.5 (CH$_3$). MS (ES+): m/z = 1004 [M + H]$^+$. IR: $\tilde{\nu}$ = 2962, 2908, 2870, 1653, 1615, 1607, 1580, 1492, 1463, 1440, 1392, 1362, 1316, 1273, 1250, 1168, 1027, 983, 963, 937, 909, 882, 874, 866, 837, 771, 749, 686, 642 cm^{-1}.

Ru$_2$[(BS2P)(CO)$_2$] (14): A solution of BS2P (200 mg, 0.20 mmol), Ru$_3$(CO)$_{12}$ (102 mg, 0.16 mmol) in toluene (5 mL) was heated under reflux for 40 h, under argon. The reaction mixture was cooled to room temperature, filtered through Celite and concentrated under reduced pressure. The resulting dark red residue was chromatographed on alumina (II−III), eluting first with CHCl$_3$ to remove a red-orange band, followed by EtOH/CHCl$_3$ (5:95) to remove a purple band. The purple band was concentrated to dryness under vacuum affording the product as a glassy purple solid. Yield: 52.0 mg (21%). ^{1}H NMR (300 MHz, [D$_6$]acetone, 22 °C): δ = 9.41 (s, 4 H), 9.14 (s, 1 H), 9.13 (s, 1 H), 7.51 (d, J = 2.7 Hz, 4 H), 7.31 (d, J = 2.4 Hz, 4 H), 1.56 (s, 36 H), 1.36 (s, 36 H). ^{13}C NMR APT (125.7 MHz, [D$_6$]acetone, 22 °C): δ = 170.9 (C), 156.9 (CH), 144.7 (C), 142.9 (C), 135.5 (C), 130.6 (CH), 130.4 (CH), 121.8 (C), 101.3 (CH), 36.7 (C), 34.5 (C), 30.3 (CH$_3$), 31.7 (CH$_3$). MS (ES+): m/z = 1258 [M$^+$]. UV/Vis (CH$_2$Cl$_2$): λ_{max} [nm] (log ε [M^{-1}cm^{-1}]) = 320 (4.58), 395 (4.62), 486 (4.47), 539sh (3.75) 568sh (4.42), 579sh (4.41). Selected IR: $\tilde{\nu}$ = 1950 (CO) cm^{-1}.

Ru$_2$[(BS2P)(CO)$_2$(py)$_2$] (15): A solution of pyridine (0.25 mL) in dichloromethane (5 mL) was treated with Ru$_2$[(BS2P)(CO)$_2$] (**14**) (35.0 mg, 0.055 mmol) and stirred at room temperature for 30 min. The solvents were evaporated and the residue applied to a small column of silica gel (1 × 2 cm) and eluted with CH$_2$Cl$_2$. The first band was collected and concentrated to dryness affording a dark purple solid. Yield: 32.0 mg (81%). ^{1}H NMR (500 MHz, CD$_2$Cl$_2$, 22 °C): δ = 9.04 (s, 2 H), 8.52 (s, 1 H), 8.51 (s, 1 H), 8.20 (m, 4 H), 7.64 (m, 2 H), 7.47 (d, J = 2.5 Hz, 4 H), 7.28 (d, J = 2.5 Hz,

4 H), 7.16 (m, 4 H), 1.56 (s, 18 H), 1.55 (s, 18 H), 1.35 (2 s, 36 H). ^{13}C NMR APT (125.7 MHz, CD$_2$Cl$_2$, 22 °C): δ = 170.3 (C), 154.3 (CH), 149.6 (CH), 149.5 (CH), 143.5 (C), 143.2 (C), 143.2 (C), 138.2 (C), 135.6 (C), 130.6 (CH), 130.1 (CH), 130.0 (CH), 124.8 (CH), 124.6 (CH), 120.9 (C), 99.7 (CH), 99.6 (CH), 36.35 (C), 34.3 (C), 31.6 (CH$_3$), 29.9 (CH$_3$). MS (ES+): m/z = 1416 [M$^+$]. Selected IR: $\tilde{\nu}$ = 1954, 1924 (CO) cm^{-1}.

Ni$_2$(BS2P): A solution of BS2P (100 mg, 0.1 mmol), Ni(OAc)$_2$(H$_2$O)$_4$ (124 mg, 0.5 mmol) in absolute EtOH (5 mL) was heated under reflux for 2 h. The reaction mixture was cooled to room temperature and the red solid was collected by filtration, washed with cold EtOH and dried under vacuum. Yield: 100 mg (89%). ^{1}H NMR (300 MHz, CD$_2$Cl$_2$, 22 °C): δ = 8.33 (s, 4 H), 8.01 (s, 2 H), 7.46 (d, J = 2.7 Hz, 4 H), 7.28 (d, J = 2.4 Hz, 4 H), 1.45 (s, 36 H), 1.36 (s, 36 H). ^{13}C NMR APT (125.7 MHz, CDCl$_3$, 22 °C): δ = 165.4 (C), 153.5 (CH), 141.5 (C), 140.9 (C), 137.4 (C), 131.2 (CH), 126.5 (CH), 119.7 (C), 98.5 (CH), 35.9 (C), 34.0 (C), 31.2 (CH$_3$), 29.7 (CH$_3$). MS (MALDI, no matrix): m/z = 1116 [M$^+$]. UV/Vis (CH$_2$Cl$_2$): λ_{max} [nm] (log ε [M^{-1}cm^{-1}]) = 268 (4.78), 322 (4.45), 374sh (4.46), 394 (4.55), 494 (4.58), 541sh (4.50). IR: $\tilde{\nu}$ = 2957, 2907, 2869, 1703, 1616, 1589, 1546, 1522, 1495, 1462, 1423, 1385, 1359, 1322, 1258, 1177, 1130, 1026, 971, 933, 916, 868, 828, 788, 749, 654, 637 cm^{-1}.

2,3,7,8-Tetraaminodibenzo-[1,4]-dioxin Tetrahydrochloride (13):$^{[14]}$ Tin metal (7.0 g, 59 mmol) was added in small portions to a suspension of 2,3,7,8-tetranitrodibenzo-[1,4]-dioxin (1.70 g, 4.7 mmol) in concentrated hydrochloric acid (25 mL). The reaction became extremely exothermic after 30 min at which point the color of the suspension changed from yellow to creamy-white. The mixture was heated under reflux for 8 h to dissolve any residual solid tin metal. The mixture was filtered leaving a white solid. The product was washed with concentrated HCl, then with EtOH and finally with Et$_2$O, and dried under vacuum. Yield: 1.35 g (74%). ^{1}H NMR (300 MHz, D$_2$O/CF$_3$CO$_2$H, 22 °C): δ = 6.63 (s). ^{13}C NMR APT (125.7 MHz, D$_2$O/CF$_3$CO$_2$H, 22 °C): δ = 140.6 (C), 123.1 (C), 112.4 (CH). MS (ES+): m/z = 244 [M − 4 HCl]$^+$.

***N*,*N*′′,*N*′′′,*N*′′′′-Tetra(3,5-di-*tert*-butylsalicylidene)dibenzo-[1,4]-dioxin-2,3,7,8-tetraamine [Bis(salophen) Precursor to 16] (BS2DP):** 3,5-Di-*tert*-butylsalicylaldehyde (750 mg, 3.20 mmol) and 2,3,7,8-tetraaminodibenzo-1,4-dioxin tetrahydrochloride (310 mg, 0.795 mmol) were heated in EtOH (18 mL) under reflux for 15 h. The solution was cooled to −10 °C and stirred at that temperature for 3 h. The yellow precipitate was collected by filtration, washed with cold EtOH and dried under vacuum. Yield: 802 mg (91%). M.p. > 350 °C. ^{1}H NMR (500 MHz, [D$_8$]THF, 22 °C): δ = 13.57 (br. s, 4 H), 8.85 (s, 4 H), 7.46 (d, J = 2.5 Hz, 4 H), 7.37 (d, J = 2.5 Hz, 4 H), 7.14 (s, 4 H), 1.45 (s, 36 H), 1.33 (s, 36 H). ^{13}C NMR APT (125.7 MHz, [D$_8$]THF, 22 °C): δ = 165.9 (CH), 159.5 (C), 141.6 (C), 141.0 (C), 140.3 (C), 137.6 (C), 128.7 (CH), 128.2 (CH), 119.7 (C), 108.2 (CH), 35.8 (C), 34.8 (C), 31.8 (CH$_3$), 30.0 (CH$_3$). MS (ES+): m/z = 1109 [M + H]$^+$. IR: $\tilde{\nu}$ = 2957, 2907, 2870, 1615, 1593, 1489, 1440, 1393, 1369, 1307, 1275, 1252, 1229, 1203, 1167, 937, 875, 861, 811, 774, 687 cm^{-1}.

Ru$_2$[(BS2DP)(CO)$_2$] (16): A solution of BS2DP (250 mg, 0.225 mmol) and Ru$_3$(CO)$_{12}$ (220 mg, 0.470 mmol) in diglyme (15 mL) was heated at 135 °C for 12 h. The reaction mixture was cooled to room temperature, filtered and concentrated to dryness under reduced pressure. The resulting dark red residue was chromatographed on alumina (II−III) eluting first with CHCl$_3$ to remove a yellow and an orange band, followed by EtOH/CHCl$_3$ (5:95) to remove a red-pink band. The latter was concentrated to dryness

under vacuum affording a glassy purple solid. Yield: 277 mg (91%). ^{1}H NMR (300 MHz, [D$_6$]acetone, 22 °C): δ = 9.20 (s, 4 H), 7.96 (s, 4 H), 7.49 (d, J = 2.7 Hz, 4 H), 7.41 (d, J = 2.4 Hz, 4 H), 1.55 (s, 36 H), 1.35 (s, 36 H). ^{13}C NMR APT (125.7 MHz, [D$_6$]acetone, 22 °C): δ = 170.6 (C), 157.1 (CH), 143.2 (C), 142.7 (C), 140.4 (C), 135.4 (C), 130.9 (CH), 130.2 (CH), 121.8 (C), 103.5 (CH), 36.6 (C), 34.5 (C), 31.7 (CH$_3$), 30.4 (CH$_3$). MS (ES+): m/z = 1363 [M$^+$]. UV/Vis (CH$_2$Cl$_2$): λ$_{max}$ [nm] (log ε [M^{-1}cm^{-1}]) = 262 (4.67), 302 (4.59), 313 (4.61), 375sh (4.59), 393 (4.64), 420sh (4.44), 507 (4.30), 550sh (4.19). Selected IR: ṽ = 1943 (CO) cm^{-1}.

Ru$_2$[(BS2DP)(CO)$_2$(py)$_2$] (17): A solution of pyridine (0.25 mL) in CH$_2$Cl$_2$ (5 mL) was treated with **16** (50 mg, 0.055 mmol) and stirred at room temperature for 30 min. The solvents were evaporated to dryness and the residue was applied to a small column of silica gel (1 × 2 cm) and eluted with CH$_2$Cl$_2$. The first band was collected and concentrated to dryness under vacuum affording a dark purple solid. Yield: 51.4 mg (81%). ^{1}H NMR (300 MHz, CD$_2$Cl$_2$, 22 °C): δ = 8.72 (s, 4 H), 8.16 (m, 4 H), 7.63 (t, J = 2.4 Hz, 2 H), 7.60 (s, 4 H), 7.43 (d, J = 2.4 Hz, 4 H), 7.14 (m, 8 H), 1.54 (s, 36 H), 1.32 (s, 36 H). ^{13}C NMR APT (125.7 MHz, CD$_2$Cl$_2$, 22 °C): δ = 170.0 (C), 154.5 (CH), 149.5 (CH), 149.5 (CH), 143.1 (C), 142.1 (C), 139.9 (C), 138.1 (CH), 135.3 (C), 130.2 (CH), 130.0 (CH), 124.7 (CH), 124.6 (CH), 120.5 (C), 102.5 (CH), 36.3 (C), 34.2 (C), 31.4 (CH$_3$), 29.9 (CH$_3$). MS (ES+): m/z = 1522 [M$^+$]. Selected IR: ṽ = 1951, 1934 (CO) cm^{-1}.

Ni$_2$(BS2DP): A solution of **BS2DP** (150 mg, 0.135 mmol) and Ni(OAc)$_2$(H$_2$O)$_4$ (168 mg, 0.676 mmol) in diglyme (15 mL) was

heated at 140 °C for 10 h under argon. The reaction mixture was cooled to room temperature and the red solution was concentrated to dryness. The residue was suspended in hot 95% EtOH (30 mL), filtered while hot and washed with EtOH. The product was then dried under vacuum. Yield: 140 mg (85%). ^{1}H NMR (300 MHz, [D$_8$]THF, 22 °C): δ = 8.40 (s, 4 H), 7.63 (s, 2 H), 7.41 (d, J = 2.7 Hz, 4 H), 7.26 (d, J = 2.4 Hz, 4 H), 1.47 (s, 36 H), 1.33 (s, 36 H). ^{13}C NMR APT (125.7 MHz, [D$_8$]THF, 22 °C): δ = 165.4 (C), 156.2 (CH), 141.0 (C), 141.0 (C), 140.1 (C), 137.2 (C), 130.9 (CH), 127.8 (CH), 120.9 (C), 103.2 (CH), 36.6 (C), 34.6 (C), 31.6 (CH$_3$), 30.3 (CH$_3$). MS (MALDI, no matrix): m/z = 1222 [M$^+$]. UV/Vis (CH$_2$Cl$_2$): λ$_{max}$ [nm] (log ε [M^{-1}cm^{-1}]) = 246sh (4.74), 270 (4.88), 304sh (4.61), 313 (4.63), 392 (4.65), 429 (4.63), 505 (4.40). IR: ṽ = 2956, 2908, 2869, 1617, 1590, 1526, 1494, 1480, 1464, 1429, 1386, 1358, 1322, 1298, 1258, 1238, 1207, 1175, 1130, 1024, 960, 934, 917, 867, 842, 787, 676, 638 cm^{-1}.

Porphyrin Complex 18a: A solution of Crossely's bis(porphyrin) (225 mg, 0.100 mmol) and Ru$_3$(CO)$_{12}$ (215 mg, 0.338 mmol) in phenol (2.0 g) was heated under reflux for 1 h, under argon. The reaction mixture was cooled to room temperature and diluted with EtOH (2 mL), and the crude product was precipitated by adding water. The crude product was collected by filtration and washed with H$_2$O/EtOH (50:50) to remove the phenol. The dark brown solid was dissolved in toluene and chromatographed on alumina (II−III) eluting first with toluene to remove an orange band, followed by CH$_2$Cl$_2$ to remove a yellow band, and then with a mixture of EtOH/CH$_2$CH$_2$ (5:95) to remove a dark brown band. The latter

Table 3. Crystallographic data for the nickel(II) analogues of **14** and **16**

	14	**16**
Empirical formula	C$_{66}$H$_{86}$N$_4$Ni$_2$O$_4$·1.4C$_3$H$_6$O·0.3CH$_2$Cl$_2$	C$_{72}$H$_{84}$N$_4$Ni$_2$O$_6$·2C$_4$H$_8$O
Molecular mass	1226.83	1367.09
Crystal size [mm]	0.38 × 0.37 × 0.33	0.28 × 0.27 × 0.08
Crystal system	orthorhombic	monoclinic
Space group	$Pbcn$ (no. 60)	$P2_1/c$ (no. 14)
a [Å]	27.4494(13)	10.6955(15)
b [Å]	21.7996(11)	14.073(2)
c [Å]	23.3535(12)	25.424(4)
β [°]		95.733
Z	8	2
V [Å^3]	13974.4(12)	3807.7(9)
Density [g cm^{-3}]	1.166	1.192
μ [mm^{-1}]	0.612	0.550
Data collection 2θ limit [°]	52.82	52.82
Total data collected	88377	16031
Independent reflections	14337	7685
Observed data with $I ≥ 2σ(I)$	10691	4974
Absorption correction method	$SADABS$	$SADABS$
Range of transmission factors	0.8236−0.8007	0.9574−0.8613
Data/restraints/parameters	14337/15[a] /740	7685/0/424
Goodness-of-fit on F^2	1.054	0.972
Final R indices [$I ≥ 2σ(I)$][b]		
$R_1 = [F_o^2 ≥ 2σ(F_o^2)]$	0.0667	0.0519
$wR_2 = [F_o^2 ≥ -3σ(F_o^2)]$	0.2130	0.1291
Largest difference peak/hole	2.350/−1.647 e·Å^{-3}	0.577/−0.273 e·Å^{-3}

[a] The following distance restraints were applied to the disordered solvent acetone and dichloromethane molecules: d(O2S−C5S) = d(O3S−C8S) = 1.22 Å; d(C4S−C5S) = d(C5S−C6S) = d(C8S−C9S) = 1.54 Å; d(O2S···C4S) = d(O2S···C6S) = d(O3S···C9S) = 2.40 Å; d(C4S···C6S) = d(C9S···C9S′) = 2.67 Å; d(Cl1S−C7S) = d(Cl2S−C7S) = d(Cl3S−C10S) = 1.80 Å; d(Cl1S···Cl2S) = d(Cl3S···Cl3S′) = 2.95 Å [primed atoms are related to unprimed ones by the crystallographic twofold rotational axis (0, y, $^1/_4$)]. [b] R_1 = Σ$||F_o| − |F_c||$/Σ$|F_o|$; wR_2 = $\{Σ[w(F_o^2 − F_c^2)^2]/Σ[w(F_o^4)]\}^{1/2}$.

was concentrated to dryness under vacuum and recrystallized from hydrous ethanol to give a brown solid. Yield 168 mg (65%). ^{1}H NMR (500 MHz, CD_2Cl_2, 22 °C): δ = 8.75 (s, 4 H), 8.72 (d, J = 5.0 Hz, 4 H), 8.63 (d, J = 5.0 Hz, 4 H), 8.53 (s, 2 H), 8.11 (m, 4 H), 8.06 (m, 4 H), 8.02 (m, 8 H), 7.99 (m, 4 H), 7.83 (m, 4 H), 1.56 (m, 144 H), 0.83 (broad, EtOH). ^{13}C NMR (125.7 MHz, CD_2Cl_2, 22 °C): δ = 153.1, 149.4, 149.3, 149.2, 147.0, 144.4, 143.0, 141.6, 141.5, 139.9, 137.1, 132.8, 131.0, 132.43, 129.5, 129.3, 129.2, 129.2, 128.9, 128.8, 125.9, 121.5, 120.3, 120.2, 35.4, 35.3, 32.3, 31.9. MS (ES+): m/z = 2508 [M − 2 EtOH]$^+$. Selected IR: ṽ = 1956 (CO) cm^{-1}.

Porphyrin(pyridine) Complex 18b: A solution of pyridine (0.25 mL) in dichloromethane (5 mL) was treated with porphyrin complex **18a** (30.0 mg, 0.012 mmol) and stirred at room temperature for 30 min. The solvents were evaporated and the residue applied to a small column of silica gel (1 × 2 cm) and eluted with CH_2Cl_2. The first band was collected and concentrated to dryness affording a dark brown solid. Yield: 20.0 mg (63%). ^{1}H NMR (300 MHz, CD_2Cl_2, 22 °C): δ = 8.69 (s, 4 H), 8.65 (d, J = 4.8, Hz 4 H), 8.57 (d, J = 4.8 Hz 4 H), 8.45 (s, 2 H), 8.05 (m, 4 H), 8.03 (m, 4 H), 7.96 (m, 8 H), 7.90 (m, 4 H), 7.81 (m, 4 H), 6.29 (t, J = 7.5 Hz, 2 H), 5.46 (t, J = 7.5 Hz, 4 H), 2.13 (d, J = 5.1 Hz, 4 H), 1.55 (s, 72 H), 1.53 (s, 36 H), 1.52 (s, 36 H). ^{13}C NMR (125.7 MHz, CD_2Cl_2, 22 °C): δ = 153.4, 149.4, 149.3, 149.3, 149.2, 149.0, 146.4, 144.8. 143.9, 142.6, 141.7, 141.7, 139.8, 136.5, 135.4, 135.4, 132.8, 132.1, 131.4, 130.0, 129.8, 129.5, 129.4, 129.0, 128.7, 128.6, 125.5, 122.6, 121.4, 120.2, 120.1, 35.4, 35.3, 32.3, 31.8. MS (ES+): m/z = 2508 [M − 2 py]$^+$. Selected IR: ṽ = 1966 (CO) cm^{-1}.

X-ray Crystallographic Study: The crystallographic data for the complexes Ni_2(BS2P), and Ni_2(BS2DP) are shown in Table 3. Crystals of Ni_2(BS2P) were grown from a mixture acetone/CH_2Cl_2 and crystals of Ni_2(BS2DP) were grown from THF. X-ray data were collected with a Bruker PLATFORM/SMART 1000 CCD at 193 K using a graphite-monochromated Mo-K_α radiation (λ = 0.71073 Å) by taking ω scans at 0.2° intervals. The structures were solved by direct methods/fragment search using the computer program DIRDIF-96 and refined by full-matrix least squares, with anisotropic displacement parameters for the non-hydrogen atoms, using the computer program SHELXL-93. Hydrogen atoms were introduced in their idealized positions as indicated by the sp^2 or sp^3 geometries of their attached carbon atoms. Crystallographic data (excluding structure factors) for the structures reported in this paper have been deposited with the Cambridge Crystallographic Data Centre as supplementary publication no. CCDC-162995 (**14**) and -162996 (**16**). Copies of the data can be obtained free of charge on application to CCDC, 12 Union Road, Cambridge CB2 1EZ, UK [Fax: (internat.) + 44-1223/336-033; E-mail: deposit@ccdc.cam.ac.uk].

[1] [1a] T. Imamura, K. Fukushima, *Coord. Chem. Rev.* **2000**, *198*, 133−156. [1b] M. J. Gunter, N. Bampos, K. D. Johnstone, J. K. M. Sanders, *New J. Chem.* **2001**, *25*, 166−173. [1c] J. E. Redman, N. Feeder, S. J. Teat, J. K. M. Sanders, *Inorg. Chem.*, in print, advance article. [1d] E. Iengo, E. Zangrando, S. Mestroni, G. Fronzoni, M. Stener, E. Alessio, *J. Chem. Soc., Dalton Trans.* **2001**, 1338−1346. [1e] U. Michelsen, C. A. Hunter, *Angew. Chem. Int. Ed.* **2000**, *39*, 764−767. [1f] R. A. Haycock, A. Yartsev, U. Michelsen, V. Sundström, C. A. Hunter, *Angew. Chem. Int. Ed.* **2000**, *39*, 3616−3619. [1g] Y. Diskin-Posner, S. Dahal, I. Goldberg, *Angew. Chem. Int. Ed.* **2000**, *39*, 1288−1292. [1h] A. Prodi, M. T. Indelli, C. J. Kleverlaan, F. Scandola, E. Alessio, T. Gianferrara, L. G. Mazilli, *Chem. Eur. J.* **1999**, *5*, 2668−2679.

[2] [2a] D. Gust, T. A. Moore, A. L. Moore, *Acc. Chem. Res.* **2001**, *34*, 40−48. [2b] M. Andersson, M. Linke, J.-C. Chambron, J. Davidsson, V. Heitz, J.-P. Sauvage, L. Hammarström, *J. Am. Chem. Soc.* **2000**, *122*, 3526−3527. [2c] L. Flamigni, I. M. Dixon, J.-P. Collin, J.-P. Sauvage, *Chem. Commun.* **2000**, 2479−2480. [2d] R. K. Lammi, A. Ambroise, T. Balasubramanian, R. W. Wagner, D. F. Bocian, D. Holten, J. S. Lindsey, *J. Am. Chem. Soc.* **2000**, *122*, 7579−7591. [2e] S. I. Yang, J. Li, H. S. Cho, D. Kim, D. F. Bocian, D. Holten, J. S. Lindsey, *J. Mater. Chem.* **2000**, *10*, 283−296. [2f] J. Brettar, J.-P. Gisselbrecht, M. Gross, N. Solladié, *Chem. Commun.*, in print, advanced article. [2g]S. Richeter, C. Jeandon, R. Ruppert, H. J. Callot, *Chem. Commun.* **2001**, 91−92. [2h] C. M. Drain, X. Shi, T. Milic, F. Nifiatis, *Chem. Commun.* **2001**, 287−288. [2i] S. Yagi, I. Yonekura, M. Awakura, M. Ezoe, T. Takagishi, *Chem. Commun.* **2001**, 557−558. [2j] A. Nakano, T. Yamazaki, Y. Nishimura, I. Yamazaki, A. Osuka, *Chem. Eur. J.* **2000**, *6*, 3254−3271. [2k] N. Aratani, A. Osuka, Y. H. Kim, D. H. Jeong, D. Kim, *Angew. Chem. Int. Ed.* **2000**, *39*, 1458−1462. [2l] K. KilsÅ, J. Kajanus, A. N. Macpherson, J. MÅrtensson, B. Albinsson, *J. Am. Chem. Soc.* **2001**, *123*, 3069−3080. [2m] H. Imahori, K. Tamaki, D. M. Guldi, C. Luo, M. Fujitsuka, O. Ito, Y. Sakata, S. Fukuzumi, *J. Am. Chem. Soc.* **2001**, *123*, 2607−2617. [2n] H. Imahori, H. Norieda, H. Yamada, Y. Nishimura, I. Yamazaki, Y. Sakata, S. Fukuzumi, *J. Am. Chem. Soc.* **2001**, *123*, 100−110. [2o] K. Ogawa, Y. Kobuke, *Angew. Chem. Int. Ed.* **2000**, *39*, 4070−4073. [2p] F. Fungo, L. A. Otero, L. Sereno, J. J. Silber, E. N. Durantini, *J. Mater. Chem.* **2000**, *10*, 645−650. [2q] Y. Sakakibara, S. Okutsu, T. Enokida, T. Tani, *Thin Solid Films* **2000**, *363*, 29−32.

[3] A. W. Herlinger, K. Ramakrishna, *Polyhedron* **1985**, *4*, 551−561.

[4] [4a] K. Chichak, N. R. Branda, *Chem. Commun.* **2000**, 1211−1212. [4b] K. Chichak, M. C. Walsh, N. R. Branda, *Chem. Commun.* **2000**, 847−848. [4c] K. Chichak, N. R. Branda, *Chem. Commun.* **1999**, 523−524.

[5] F. Calderazzo, C. Floriani, R. Henzi, F. L'Eplattenier, *J. Chem. Soc. A* **1969**, 1378−1386.

[6] N. Farrell, M. N. De Oliveira Bastos, A. A. Neves, *Polyhedron* **1983**, *2*, 1243−1246.

[7] M. M. Taqui Khan, Z. A. Shaikh, *Ind. J. Chem.* **1992**, *31A*, 191−194.

[8] J. Wöltinger, J.-E. Bäckvall, Á. Zsigmond, *Chem. Eur. J.* **1999**, *5*, 1460−1467.

[9] A. L. Singer, D. A. Atwood, *Inorg. Chim. Acta* **1998**, *277*, 157−162.

[10] For a good discussion of pyridine as a π-acid in ruthenium(II) carbonyl complexes, see: R.-J. Cheng, S.-H. Lin, H.-M. Mo, *Organometallics* **1997**, *16*, 2121−2126.

[11] E. C. Constable, A. M. W. Cargrill Thompson, *J. Chem. Soc., Dalton Trans.* **1994**, 1409−1418.

[12] E. C. Constable, A. M. W. Cargrill Thompson, *J. Chem. Soc., Dalton Trans.* **1992**, 2947−2950.

[13] R. J. Morgan, A. D. Baker, *J. Org. Chem.* **1990**, *55*, 1986−1993.

[14] For the synthesis of the dibenzodioxin fragment, see: [14a] R. C. Cambie, S. J. Janssen, P. S. Rutledge, P. D. Woodgate, *J. Organomet. Chem.* **1991**, *420*, 387−418. For the nitration of

the dibenzodioxin fragment, see: [14b] H. Gilman, J. J. Dietrich, *J. Am. Chem. Soc.* **1958**, *80*, 366−368. For the reduction of the nitrated compound, see: [14c] W. Knobloch, H. Niedrich, *Chem. Ber.* **1958**, *91*, 2562−2566.

[15] A pair of *cis* and *trans* diastereomers has also been reported for multimetallic porphyrin monomers: S. C. Darling, P. K. Y. Goh, N. Bampos, N. Feeder, M. Montalti, L. Prodi, B. F. G. Johnson, J. K. M. Sanders, *Chem. Commun.* **1998**, 2031−2032.

[16] M. J. Crossley, P. L. Burn, *J. Chem. Soc., Chem. Commun.* **1987**, 39−40.

[17] V. Promarak, P. L. Burn, *J. Chem. Soc., Perkin Trans. 1* **2001**, 14−20.

[18] [18a] A. M. El-Hendawy, A. H. Alkubaisi, A. El-Ghany El-Kourashy, M. M. Shanab, *Polyhedron* **1993**, *12*, 2343−2350. [18b] M. M. Taqui Khan, Z. A. Shaikh, R. I. Kureshy, A. B. Boricha, *Polyhedron* **1992**, *11*, 91−100. [18c] M. M. Taqui Khan, D. Srinivas, R. I. Kureshy, N. H. Khan, *Inorg. Chem.* **1990**, *29*, 2320−2326.